

## Relationship between transmission/reception conditions of high-frequency plane wave compounding and evaluation accuracy of extended amplitude envelope statistics

Taisei Higa<sup>1†</sup>, Jeffrey A. Ketterling<sup>2</sup>, Jonathan Mamou<sup>2</sup>, Cameron Hoering<sup>2</sup>, Daniel H. Gross<sup>2</sup>, Tingzhen Zhang<sup>1</sup>, Mami Shirai<sup>3</sup>, Shinnosuke Hirata<sup>4</sup>, Kenji Yoshida<sup>4</sup>, Tadashi Yamaguchi<sup>4\*</sup> (<sup>1</sup> Grad. School Sci. and Eng., Chiba Univ.; <sup>2</sup>Radiology, Weill Cornell Medicine; <sup>3</sup>Eng. Chiba Univ.; <sup>4</sup>Center for Frontier Medical Engineering, Chiba Univ.)

### 1. Introduction

Amplitude envelope statistics of echo signals is one of the methods for quantitative evaluation of biological tissue properties such as the liver. The Double Nakagami (DN) Model, which combines two Nakagami distributions, has been proposed, and study using single concave transducer at 15 to 25 MHz showed that it was possible to evaluate fatty characteristics in the fatty liver animals<sup>1)</sup>. However, evaluation using a high-frequency array sensor is necessary for application in current clinical situations, in which case the influence of the sound field characteristics and ultrasound transmission and reception conditions by the system must be fully considered<sup>2)</sup>.

In this study, a fatty liver mimicking phantom was observed using several types of high-frequency linear array probes, and amplitude envelopment statistics were evaluated using the DN Model to confirm the relationship between the scatterer structure and evaluation parameters and the influence of sound field characteristics on evaluation accuracy.

### 2. Method

#### 2.1 Data Acquisition

The measurement system used Vantage 256 (Verasonics) and high-frequency linear array probes with different frequency bands (L22-14v, L35-16vX, L38-22v (Verasonics), L39-21gD (Daxsonics), MS550D (Fujifilm)). The center frequency of each probe was 16, 27, 31, 31, and 38 MHz, respectively, and the sampling frequency during observation was set to four times the center frequency. Echo data were obtained by steering plane waves at 11 angles between -15° and 15°, by transmitting and receiving at each angle, and then processed by compound plane wave imaging (CPWI)<sup>3)</sup> using synthetic aperture and compounded data for analysis.

A fatty liver phantom, which contains two kind of scatterers, was prepared by mixing a 20 μm

diameter scatterer (MX-2000, Soken) simulating strong scatterers as fat droplets and 5 μm diameter weak scatterers (Orgasol 2001 UD NAT1, Arkema) simulating the normal liver into agar gel. The volume fraction of both scatterers were same as 0.25%. These values were determined as the probability density function of echo from fat droplet components becomes under the condition of pre-Rayleigh.

#### 2.2 Amplitude Envelope Statistics Model

The Nakagami distribution is expressed as follows (1).

$$p(x) = \frac{2\mu^\mu x^{2\mu-1}}{\Gamma(\mu)\omega^\mu} \exp\left\{-\left(\frac{\mu}{\omega}\right)x^2\right\} \quad (1)$$

$x$  is the amplitude envelope,  $\Gamma$  is the gamma function, and  $\mu$  and  $\omega$  are parameters of the scatterer number density and echo signal power, respectively.  $\mu$  is Nakagami parameter and is classified as pre-Rayleigh when  $\mu < 1$ , Rayleigh when  $\mu = 1$ , and post-Rayleigh when  $\mu > 1$ <sup>4)</sup>.

The DN Model combines two Nakagami functions and assumes that the echo signal from the fatty liver contains both normal liver tissue and fat droplet components, and is expressed as

$$p_{mix}(x) = (1 - \alpha)p_L(x|\mu_L, \omega_L) + \alpha p_F(x|\mu_F, \omega_F) \quad (2)$$

$p_L$  and  $p_F$  are defined as the probability density functions of the echo signals of normal liver tissue including luminal structures and fat droplets as the main scattering sources.  $\mu_L$  and  $\mu_F$  correspond to the number density of normal liver tissue and fat droplets, while  $(1 - \alpha)\omega_L$  and  $\alpha\omega_F$  are the parameters for the intensity of echo signals from normal liver tissue and fat droplets respectively. Each parameter of the DN Model was determined by optimization based on the Kullback-Leibler information content in Equation (3).

$$D_{KL}(p||p_{mix}) = \sum_{i=0}^{\infty} q(x_i) \log \frac{q(x_i)}{p(x_i)} \quad (3)$$

The DN parameter,  $\alpha$ ,  $\mu_L$ ,  $\mu_F$ ,  $\omega_F$ , was optimized using the MATLAB (The MathWorks

E-mail: <sup>†</sup>thiga@chiba-u.jp, <sup>\*</sup>yamaguchi@faculty.chiba-u.jp

Inc.) library function, “fminsearch”, with the cost function,  $D_{KL}$ . Considering the ratio of echo signal intensity from fat droplets and normal liver components,  $\omega_L < \omega_F$  was adopted as a constraint condition for the analysis.

### 3. Results and Discussion

#### 3.1 Classification evaluation by amplitude envelope statistics

Figure 1 shows the MS550D echo data (B-mode) superimposed with (a)  $\mu_F$ , the number density of fat droplet components, and (b)  $\alpha\omega_F$ , the signal intensity of fat droplet components, for (i) the normal liver phantom and (ii) the fat liver phantom. In both phantoms,  $\mu_F$  was evaluated to be smaller than 1 at all depths, which is consistent with the expected scatterer structure. Compared to Fig. 1(b-i),  $\alpha\omega_F$ , which corresponds to the scattering intensity from fat droplets, is higher in the entire evaluation region in Fig. 1(b-ii), and the base 5  $\mu\text{m}$  weak scatterer (liver) and the 20  $\mu\text{m}$  strong scatterer (fat) are discriminated.

#### 3.2 Relationship between probe characteristics and evaluation accuracy

Figure 2 illustrates the results of the evaluation of the data acquired with the L22-14v with a point spread function (PSF) of 256  $\mu\text{m}$  depth  $\times$  220  $\mu\text{m}$  azimuth and the MS550D with a PSF of 113  $\mu\text{m}$   $\times$  94  $\mu\text{m}$ . The spatial resolution of the MS550D is higher than that of the L22-14v. For MS550D, which has a high spatial resolution, the distribution transitions to a region where  $\mu_F$  is small and  $\alpha\omega_F$  is large compared to L22-14v. In Fig. 2(b), the probability of the percentage of echoes from the fat component (strong scatterer) in each pixel component is superimposed on the B-mode. Compared to L22-14v, the high-dispersion component of MS550D is evaluated as an independent scatterer signal rather than an interference component.

### 4. Conclusions

The fat component evaluation results were compared between five different high-frequency linear array probes with center frequencies ranging from 15 MHz to 40 MHz in combination with the DN Model. The low-resolution probe evaluated both strong and weak scatterers as well as interference signals between strong scatterers as fat components, while the high-resolution probe evaluated only strong scatterers as fat components. It is suggesting the possibility of fat volume quantification reflecting microscopic tissue structure with high frequency high-resolution probe and DN model. In future works, we will evaluate fat content using animal and clinical data.

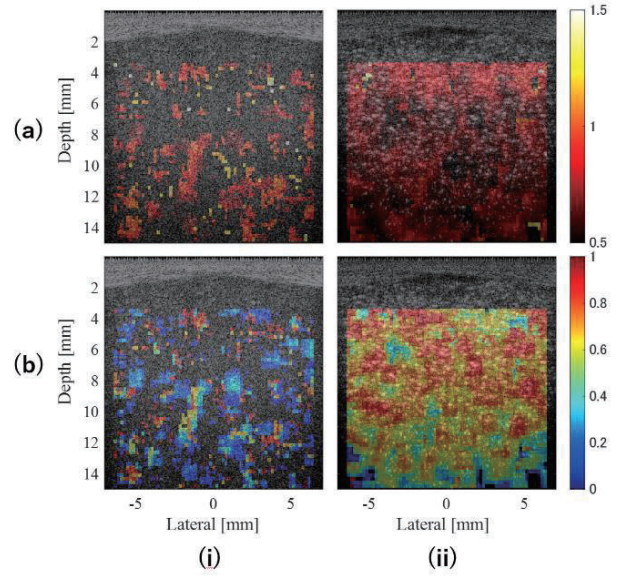


Fig. 1 Number density (a) and signal intensity (b) of  $p_L$  components of healthy liver and fatty liver phantoms evaluated by DN Model

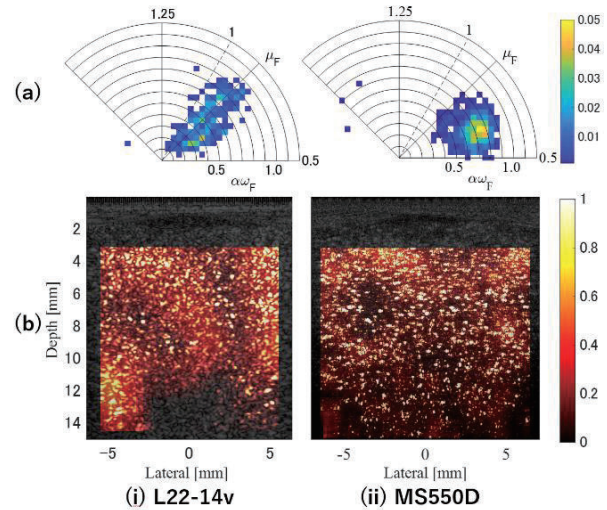


Fig. 2 Probability density distribution of evaluation parameters and probability images of fat droplet components for data measured with L22-14v and MS550D.

### Acknowledgment

This research was partly supported by KAKENHI Grant Numbers 22KK0179, 23H03758 and Chiba University Institute for Advanced Academic Research.

### References

- 1) K. Tamura et al., JJAP 59, SKKE23, 2020.
- 2) Y. Ujihara et al., JJAP 62, SJ1043, 2023.
- 3) G. Montaldo, IEEE TUFFC, 56 (2009).
- 4) P. M. Shankar, IEEE TUFFC, 47 (2000).